Solid-State Reactivity and Single-Crystal Structure Studies. The Case of *diag*−*lat* Isomerization in [Re(η^5-C_5H_4Me)(CO)(P(OPh_3)Br_2] and [Re(η^5-$C_5H_4{}^tBu$)$(CO)_2Br_2$]

Jeremy M. Smith, Lin Cheng, Neil J. Coville,* Jurgen Schulte, Priscilla S. Dimpe, Michael S. Adsetts, Leanne M. Cook, Jan C. A. Boeyens, and Demetrius C. Levendis*

Chemistry Department, University of the Witwatersrand, PO Wits 2050, South Africa

Received December 6, 1999

The complex [Re(η^5-C_5H_4Me)(CO)(P(OPh_3)Br_2] (**1**) isomerizes from the *diag*→*lat* (*trans*→*cis*) isomer in the solid state, while [Re(η^5-$C_5H_4{}^tBu$)$(CO)_2Br_2$] (**2**) does not isomerize, although **2** is found to isomerize in the melt. Both complexes isomerize from the *lat*→*diag* isomer in solution. The crystal structures of both isomers of **1** and **2** have been determined by single-crystal X-ray diffraction. The crystal structures of **1** are analyzed to determine the structural forces driving the solid-state isomerization. For **2**, the crystal structures are analyzed and compared with those of [Re(η^5-C_5H_4Me)$(CO)_2Br_2$] (**3**), which does isomerize in the solid state.

Introduction

Crystal engineering is a "strategy to construct crystals with a purpose".[1,2] Clearly, when molecules or ions are used as the building blocks of the crystal, the intermolecular interactions holding these building blocks together need to be recognized. Whether the end goal is the synthesis of crystals with specific characteristics or reactivity, recognition of these intermolecular interactions is of utmost importance[1−3] This is an issue we address in this paper.

Some years ago we made the interesting discovery of a complex that shows phase-dependent isomerization behavior. It was found that the complex, *diag*-[Re(η^5-C_5H_4Me)$(CO)_2Br_2$] (**3**), isomerized to the lateral isomer in the solid state, opposite of the direction of the solution isomerization reaction (Figure 1). Similar rhenium complexes bearing other substituents on the cyclopentadienyl ring do not show this solid-state phenomenon, although isomerization does occur in the melt.[4,5] However, complexes in which one of the carbonyl groups had been substituted by another ligand did isomerize in the solid state, regardless of the ring substituent.[6,7]

Emerging from these studies is the observation that isomerization always occurs from the low to the high melting point isomer; if the two melting points are close, isomerization occurs in the melt. However, the direction of isomerization in solution, the melt, and the solid state do not appear to be related in an obvious way.[4−8] It is worth noting that there are examples of other "four-legged piano stool" complexes of molybdenum and tungsten that isomerize in the solid state.[9−11]

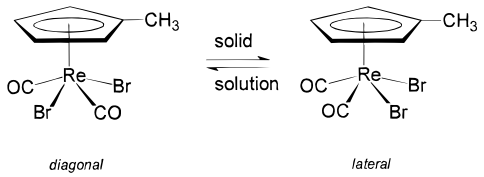

Figure 1. Isomerization behavior of [Re(η^5-C_5H_4R)(L)(CO)-Br_2] complexes.

Crystallographic and molecular modeling analyses of both isomers of **3** did not identify inter- or intramolecular interactions that could provide the driving force for the isomerization reaction. However, indirect evidence exists that suggests that a high-temperature crystal modification of the *diag* isomer, which does not pack efficiently in the crystal, spontaneously rearranges to the *lat* isomer.[12] The mechanism by which the isomerization occurs in the solid state is still unclear. A structure correlation analysis of related structures suggests a combined Berry−turnstile mechanism for the isomerization; this is not inconsistent with the solid-state structures.[12,13]

(1) Braga, D.; Grepioni, F. *Coord. Chem. Rev.* **1999**, *183*, 19−41.
(2) Braga, D.; Grepioni, F.; Desiraju, G. R. *Chem. Rev.* **1998**, *98*, 1375−1405.
(3) Braga, D.; Scaccianoce, L.; Grepioni, F.; Draper, S. M. *Organometallics* **1996**, *15*, 4675−4677.
(4) Cheng, L.; Coville, N. J. *Organometallics* **1996**, *15*, 867−871.
(5) Cheng, L.; Carlton, L.; Coville, N. J. *S. Afr. J. Chem.* **1998**, *51*, 127−131.
(6) Cheng, L.; Coville, N. J. *J. Organomet. Chem.* **1998**, *556*, 111−118.
(7) Cheng, L.; Coville, N. J. *Thermochim. Acta* **1998**, *319*, 27−32.
(8) Coville, N. J.; Cheng, L. *J. Organomet. Chem.* **1998**, *571*, 149−169.
(9) Beach, D. L.; Dattilo, M.; Barnett, K. W. *J. Organomet. Chem.* **1977**, *140*, 47−51.
(10) Filippou, A. C.; Winter, J. G.; Feist, M.; Kociok-Köhn, G.; Hinz, I. *Polyhedron* **1998**, *17*, 1103−1114.
(11) Mamba, B. B.; Cheng, L.; Eke, B.; Morar, J.; Ngoma, B.; Coville, N. J. Unpublished results.
(12) Boeyens, J. C. A.; Cheng, L.; Coville, N. J.; Levendis, D. C.; McIntosh, K. *J. Chem. Crystallogr.* **1998**, *28*, 185−191.
(13) Smith, J. M.; Coville, N. J. *Organometallics* **1996**, *15*, 3388−3392.

10.1021/om990959z CCC: $19.00
Publication on Web 05/31/2000

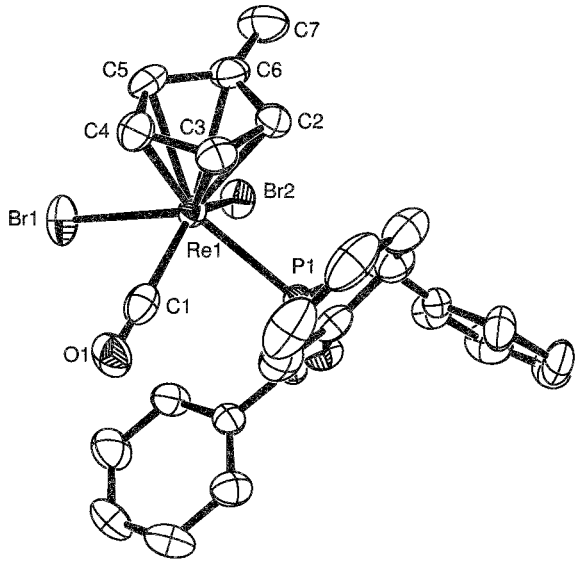

Figure 2. ORTEP diagram and numbering scheme of *diag*-[Re(η^5-C_5H_4Me)(P(OPh)$_3$)(CO)Br_2], **1a**. Hydrogen atoms omitted for clarity. Thermal ellipsoids shown at 50% probability.

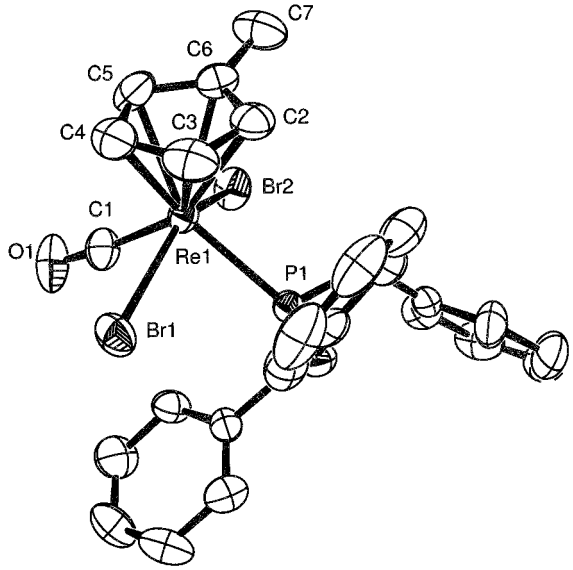

Figure 3. ORTEP diagram and numbering scheme of *lat*-[Re(η^5-C_5H_4Me)(P(OPh)$_3$)(CO)Br_2], **1b**. Hydrogen atoms omitted for clarity. Thermal ellipsoids shown at 50% probability.

As indicated above, substituted complexes of the type [Re(η^5-C_5H_4R)(L)(CO)X_2] also isomerize in the solid state, while complexes [Re(η^5-C_5H_4R)(CO)$_2Br_2$] (R ≠ Me) do not. We thus thought it would be instructive to examine the structures of both types of complex in the solid state and, by comparison of these structures, determine the forces that drive the isomerization reaction. In this paper we present such a crystallographic structural analysis, one for a complex that isomerizes in the solid state ([Re(η^5-C_5H_4Me)(P(OPh)$_3$)(CO)Br_2], **1**) and one for a complex that does not ([Re(η^5-$C_5H_4{}^tBu$)-(CO)$_2Br_2$], **2**).

Two other inorganic/organometallic complexes have been reported to isomerize with retention of the crystal form in the solid state: linkage isomerization of the nitro ligand in [$Co(NH_3)_5NO_2$][$Cl(NO_3)$][14,15] and $\beta-\alpha$ photoisomerization of cobaloxime complexes.[16,17] These studies indicate that crystallographic analyses permit an understanding of the isomerization process. It can thus be anticipated that our study should also provide valuable information on the solid-state isomerization reaction.

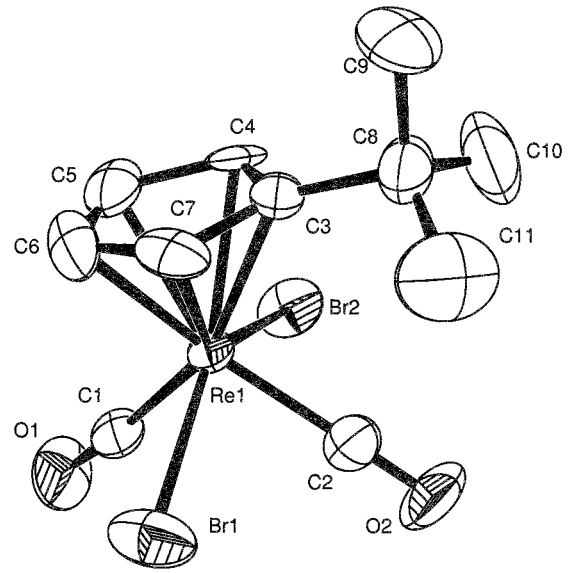

Figure 4. ORTEP diagram and numbering scheme of *diag*-[Re(η^5-$C_5H_4{}^tBu$)(CO)$_2Br_2$], **2a**. Hydrogen atoms omitted for clarity. Thermal ellipsoids shown at 50% probability.

Results and Discussion

The molecular structures of both the diagonal and lateral isomers of **1**[6] and **2**,[4] previously determined spectroscopically, are confirmed by X-ray crystallography. The atomic numbering scheme of the complexes is shown in the ORTEP diagrams (Figures 2−5). Selected bond lengths and angles of complexes **1a** (*diag*) and **1b** (*lat*) are listed in Table 1; for complexes **2a** (*diag*) and **2b** (*lat*) they are listed in Table 2.

As expected, both isomers of complex **1** adopt a distorted pseudo square pyramidal geometry. As far as we are aware, no crystal structures of rhenium phosphite complexes have been reported; however the Re−P bond length of **1a** (2.377(1) Å) is shorter than those in four-legged piano stool complexes of rhenium containing phosphines or phosphonates. In [Re(η^5-C_5Me_4Et)(PMe_3)$_2$-Cl_2] the two Re−P bond lengths are 2.406(1) and 2.409-(1) Å,[18] while in [Re(η^5-C_5Me_5)(CO)$_2$(PO(OMe)$_2$][I] the Re−P bond length is 2.417(5) Å.[19] The Re−Br, Re−CO, Re−cen, and P−O bond distances do not show unusual deviations from the corresponding distances in previously determined structures.[20] In general, the *lat* isomer

(14) Boldyreva, E.; Kivikoski, J.; Howard, J. A. K. *Acta Crystallogr.* **1997**, *B35*, 294−404.
(15) Boldyreva, E. V.; Naumov, D. Y.; Ahsbahs, H. *Acta Crystallogr.* **1999**, *A55 Supplement*, Abstract P11.19.001.
(16) Sekine, A.; Tatsuki, H.; Ohashi, Y. *J. Organomet. Chem.* **1997**, *536*−*537*, 389−398.
(17) Ohhara, T.; Harada, J.; Ohashi, Y.; Tanaka, I.; Kumuzawa, S.; Niimura, N. *Acta Crystallogr.* **1999**, *A55 Supplement*, Abstract P05.06.011.
(18) Herrmann, W. A.; Fischer, R. A.; Felixberger, J. K.; Paciello, R. A.; Kiprof, P.; Herdtweck, E. *Z. Naturforsch.* **1988**, *B43*, 1391−1404.
(19) Einstein, F. W. B.; Rickard, C. E. F.; Klahn, H.; Leiva, C. *Acta Crystallogr.* **1991**, *C47*, 862−864.

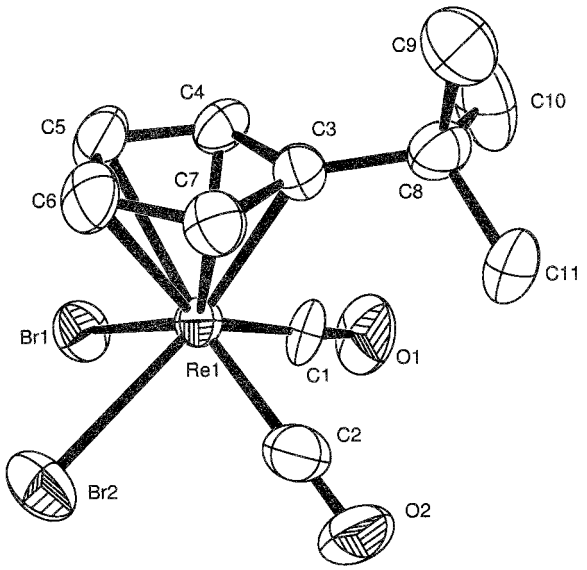

Figure 5. ORTEP diagram and numbering scheme of *lat*-[Re(η^5-$C_5H_4{}^tBu$)$(CO)_2Br_2$], **2b**. Hydrogen atoms omitted for clarity. Thermal ellipsoids shown at 50% probability.

Table 1. Selected Bond Lengths (Å) and Angles (deg) for Complexes [Re(η^5-C_5H_4Me)(CO)(P(OPh)$_3$)Br_2], 1a and 1b

	1a, *diag*	**1b**, *lat*
Re(1)−P(1)	2.3772(13)	2.3341(11)
Re(1)−Br(1)	2.6097(6)	2.5986(6)
Re(1)−Br(2)	2.5903(5)	2.6013(5)
Re(1)−C(1)	1.9165(6)	1.931(6)
Re(1)−cen[a]	1.9400(2)	1.9529(2)
C(1)−O(1)	1.158(7)	1.077(6)
C(6)−C(7)	1.485(9)	1.488(8)
P(1)−O(2)	1.592(3)	1.591(3)
P(1)−O(3)	1.592(4)	1.593(3)
P(1)−O(4)	1.609(4)	1.608(3)
Br(1)−Re(1)−Br(2)	138.80(2)	79.167(18)
Br(1)−Re(1)−C(1)	76.36(18)	77.47(15)
Br(1)−Re(1)−P(1)	81.49(3)	127.77(3)
Br(2)−Re(1)−C(1)	75.62(17)	127.34(15)
Br(2)−Re(1)−P(1)	79.80(3)	77.53(3)
C(1)−Re(1)−P(1)	109.00(2)	80.49(15)

[a] cen = cyclopentadienyl ring centroid.

Table 2. Selected Bond Lengths (Å) and Angles (deg) for Complexes [Re(η^5-$C_5H_4{}^tBu$)$(CO)_2Br_2$], 2a and 2b

	2a, *diag*	**2b**, *lat*
Re(1)−Br(1)	2.5882(13)	2.5927(13)
Re(1)−Br(2)	2.5883(14)	2.5973(14)
Re(1)−C(1)	1.940(13)	1.935(13)
Re(1)−C(2)	1.963(14)	1.910(15)
Re(1)−cen[a]	1.9198(4)	1.9458(4)
C(3)−C(8)	1.53(2)	1.535(18)
C(1)−O(1)	1.136(14)	1.112(15)
C(2)−O(2)	1.120(14)	1.139(17)
Br(1)−Re(1)−Br(2)	139.97(5)	80.67(5)
Br(1)−Re(1)−C(1)	78.4(4)	75.8(3)
Br(1)−Re(1)−C(2)	76.9(3)	122.7(4)
Br(2)−Re(1)−C(1)	77.0(4)	127.5(4)
Br(2)−Re(1)−C(2)	78.1(4)	76.1(4)
C(1)−Re(1)−C(2)	102.2(5)	78.5(6)

[a] cen = cyclopentadienyl ring centroid.

1b has bond lengths similar to **1a**, although the Re(1)−P(1) bond length is noticeably shorter in **1b** (2.334(1) Å), consistent with the CO having a greater *trans* influence than Br. Interestingly, in both isomers the P(1)−O(4) bond is slightly longer than the other two P−O bond lengths.

For both isomers, the lateral angles around the rhenium atom are all similar. It is noticeable that in **1a** the *trans* Br(1)−Re(1)−Br(2) bond angle is substantially larger than the *trans* C(1)−Re(1)−P(1) bond angle, while the corresponding bond angles in **1b**, C(1)−Re(1)−Br(2) and P(1)−Re(1)−Br(1), are the same within experimental error, at 127°. This effect has been rationalized in terms of a π-bonding "angular *trans* influence"[21] and a σ-bonding model.[22]

More interesting are the crystallographic features observed in the crystal packing diagrams of **1a** and **1b** (Figures 6 and 7). Both isomers have exactly the same packing arrangements, with the phenyl rings "interlocked" with those of neighboring molecules. A significant cavity is formed between rows of adjacent molecules as a result of this interlocking. Thus, one would expect minimal hindrance toward the movement of the other basal ligands when *diag*−*lat* isomerization occurs. While the *intermolecular* interactions in the bulk of the material are nearly the same in both isomers and by themselves do not explain why the *lat* isomer should be energetically preferred, we note that the density of the *lat* isomer is about 0.5% greater than the *diag*. As a result of the same packing arrangements, both isomers crystallize in the monoclinic $P2_1/c$ space group with the same unit cell (i.e., they appear to be isomorphous). This observation, plus the minimal hindrance toward movement of the basal ligands, would appear to explain why no cracking of the crystal occurs in the solid-state isomerization reaction of this complex,[4] although it is possible to observe significant changes in atomic positions without crystal shattering.[23]

The crystal structures of **2a** and **2b** do not show any particularly unusual features. As might be expected, the bond lengths around rhenium in both isomers are very similar to those of **3**[12] and do not show any unusual deviations from previously reported structures.[20] The bond angles around the rhenium atom show features similar to those of **1** and **3**.[12] However, as compared with the structure of *diag*-**3**, **2a** shows a different orientation of the basal ligand set relative to the cyclopentadienyl ring. That is, while in **2a** the cyclopentadienyl ring substituent eclipses one of the carbonyl ligands (C(8)−C(3)−Re(1)−C(2) = 2.86°), in *diag*-**3** the ring is staggered with respect to the basal ligands (C(8)−C(3)−Re(1)−C(2) = −39.43°).[12] The relative orientations of these ligands in **2b** is similar to that in *lat*-**3**.[12]

To try understand why solid-state isomerization is not observed for **2**, we compare the crystal packing of these complexes with those observed for **3**, which does isomerize. Not unexpectedly, the packing of complexes **2** is different from those of **3**. In **2a** all molecules are aligned in a head-to-tail manner, with the direction of every two molecular layers opposite that of the neighboring two layers (Figure 8). There are no large cavities between molecules, since the *tert*-butyl ring substituent on one

(20) Orpen, A. G.; Brammer, L.; Allen, F. H.; Kennard, O.; Watson, D. G.; Taylor, R. *J. Chem. Soc., Dalton Trans.* **1989**, S1−S83.

(21) Poli, R. *Organometallics* **1990**, *9*, 1892−1900.
(22) Lin, Z.; Hall, M. B. *Organometallics* **1993**, *12*, 19−23.
(23) Miller, E. J.; Brill, T. B.; Rheingold, A. L.; Fultz, W. C. *J. Am. Chem. Soc.* **1983**, *105*, 7580−7584.

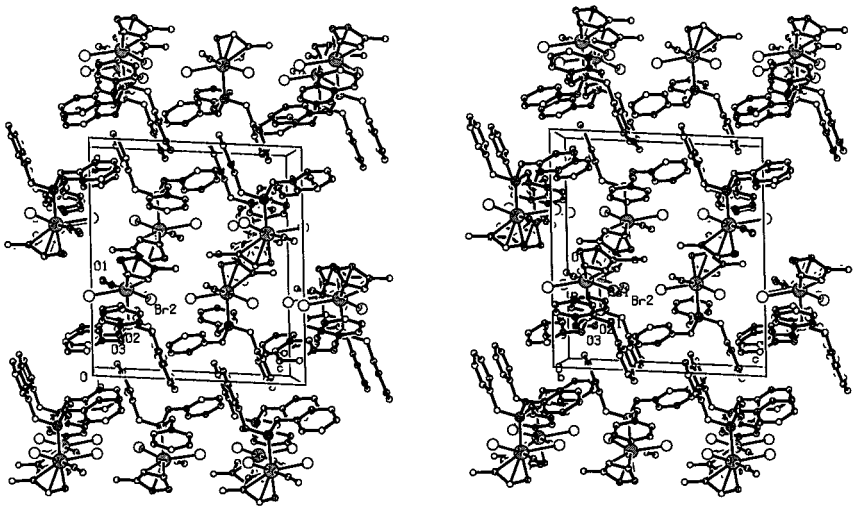

Figure 6. Stereoscopic packing diagram of **1a** (*diag*). Hydrogens omitted for clarity.

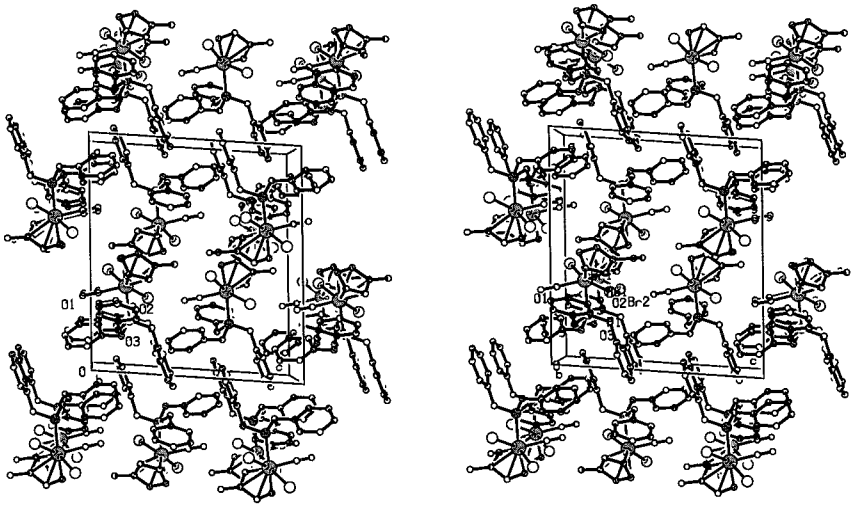

Figure 7. Stereoscopic packing diagram of **1b** (*lat*). Hydrogens omitted for clarity.

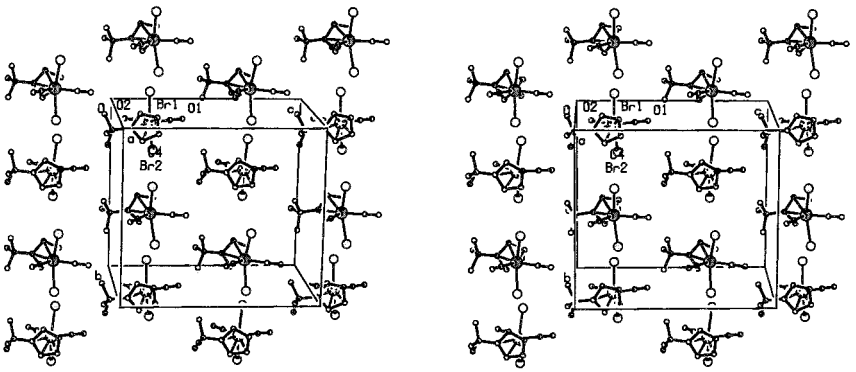

Figure 8. Stereoscopic packing diagram of **2a** (*diag*). Hydrogens omitted for clarity.

molecule is oriented between the bromine atoms of an adjacent molecule. This may inhibit basal ligand rotation around the rhenium atom. It is noteworthy that a significant cavity between adjacent molecules is observed in *diag*-**3** (Figure 9). Similarly to **1**, the *tert*-butyl substituent of ring substituent **2a** may also lock in the position of the molecules, but this may prevent solid-state isomerization, since the change in space group from the *diag* to the *lat* isomer would require *translational motion of the entire molecule*. In **2b** the molecules are also layered, but in this case there are alternating polar and nonpolar interfaces between the two layers (Figure 10). A search for intermolecular interactions failed to detect significant differences in observed nonbonded contacts in the crystal structures of the two isomers (Table 3).

From the results of this and other studies,[12] it is clear that the forces driving the solid-state *diag*−*lat* isomerization are subtle. For complex **1** the packing of the crystal appears to make isomerization facile, but there do not appear to be any interactions in the two crystals that would lead to one isomer being favored over the

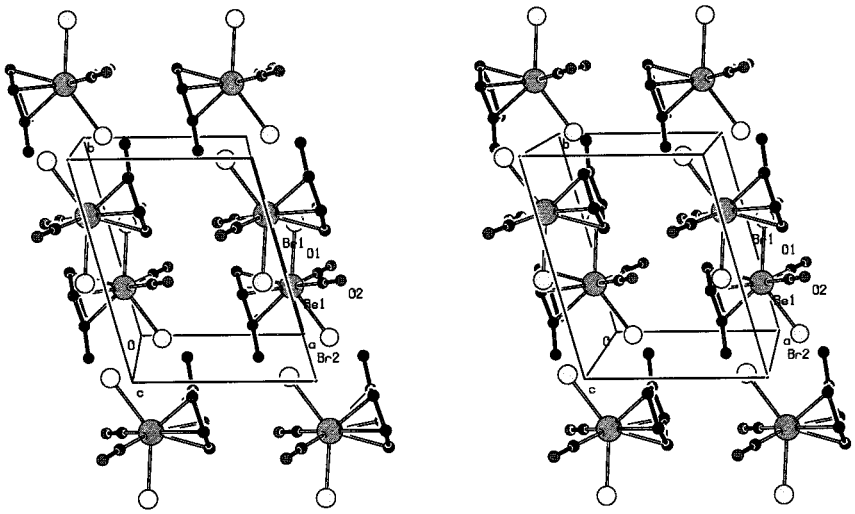

Figure 9. Stereoscopic packing diagram of *diag*-**3**. Hydrogens omitted for clarity.

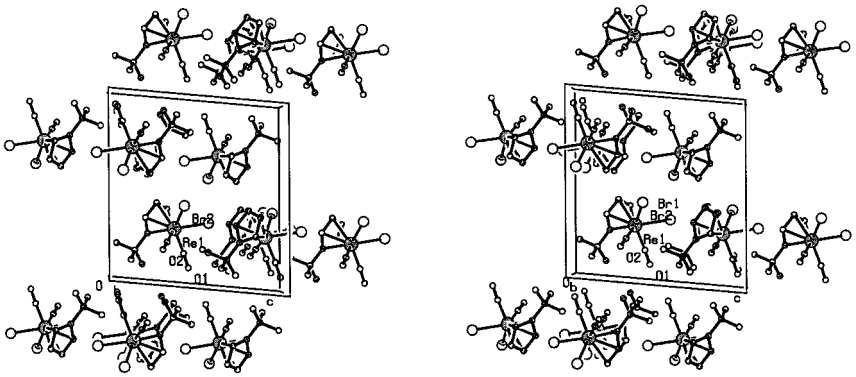

Figure 10. Stereoscopic packing diagram of **2b** (*lat*). Hydrogens omitted for clarity.

Table 3. Selected Intermolecular Contacts (Å) in [Re(η^5-C_5H_4Me)(CO)(P(OPh_3)Br_2] 1 and [Re(η^5-$C_5H_4{}^tBu$)$(CO)_2Br_2$] 2

1a, *diag*			**1b**, *lat*		
contact	distance	symmetry operation	contact	distance	symmetry operation
Br(1)−C(2)	3.938	$x, 1/2 - y, -1/2 + z$	Br(1)−H(4)	2.839	$1 - x, -y, -z$
Br(2)−C(44)	4.236	$x, -1 + y, z$			
2a, *diag*			**2b**, *lat*		
contact	distance	symmetry operation	contact	distance	symmetry operation
Br(1)−Br(2)	3.703	$-x, -1/2 + y, 1/2 - z$	Br(1)−H(6)	2.981	$1 - x, 1 - y, 1 - z$
Br(2)−H(4)	3.026	$1/2 - x, -1/2 + y, z$	Br(2)−Br(2)	3.771	$1 - x, 2 - y, 1 - z$
Br(2)−Br(1)	3.703	$-x, 1/2 + y, 1/2 - z$	O(1)−O(1)	3.035	$x, 1/2 - y, -1/2 + z$

other. The previous suggestion of a high-temperature form of the *diag* isomer rearranging spontaneously to the more symmetrical *lat* form[12] does not seem likely for **1**, as the isomers appear to be isomorphous. While the difference in cavity size between complex **2**, which does not isomerize in the solid state, and **3**, which does, may possibly explain solid-state behavior, there do not appear to be any significant differences in intermolecular interactions that would favor one isomer over another. Thus at present, we are unable to predict *a priori* from the crystal structure whether a complex will isomerize in the solid state or not. As we have noted, it is possible that the size[24] and shape[16] of the cavity may be important in allowing isomerization to occur. However, calculation of the percentage void in the unit cells of **1a**, **2a**, and **3** failed to reveal any appreciable differences.

Indeed, the only clear principle emerging from our studies is the rather unglamorous observation that isomerization in the solid state proceeds from the isomer with the lower melting point to the isomer with the higher melting point. In the cases where isomerization does occur, it appears to occur with increase in density. Although our results have not been directed to finding a potential isomerization mechanism, it is to be noted that the crystallographic packing of **1** is consistent with solid-state isomerization by a turnstile mechanism[13] or even the movement of just two ligands. The interlocking phenyl groups would most likely preclude extensive movement of the phosphite ligand, and the bulky cyclopentadienyl ring is also unlikely to undergo extensive movement in the solid state. However, as yet we

(24) Ohashi, Y. *Acc. Chem. Res.* **1988**, *21*, 268−274.

Table 4. Crystal Data and Details of Structure Refinement for Complexes 1 and 2

	1a, *diag*	**1b**, *lat*	**2a**, *diag*	**2b**, *lat*
empirical formula	$C_{25}H_{22}Br_2O_4PRe$	$C_{25}H_{22}Br_2O_4PRe$	$C_{11}H_{13}Br_2O_2Re$	$C_{11}H_{13}Br_2O_2Re$
fw	763.42	763.42	523.23	523.23
temp (K)	296(2)	296(2)	293(2)	296(2)
wavelength (Å)	0.71073	0.71073	0.71073	0.71073
cryst syst	monoclinic	monoclinic	orthorhombic	monoclinic
space group	$P2_1/c$	$P2_1/c$	$Pbca$	$P2_1/a$
unit cell dimens	a = 15.8117(7) Å, α = 90°	a = 15.9490(7) Å, α = 90°	a = 12.5359(6) Å, α = 90°	a = 13.5376(8) Å, α = 90°
	b = 11.1102(5) Å, β = 93.632(1)°	b = 10.8893(5) Å, β = 94.534(1)°	b = 14.2599(7) Å, β = 90°	b = 8.0422(5) Å, β = 95.454°
	c = 14.1533(6) Å, γ = 90°	c = 14.2549(7) Å, γ = 90°	c = 15.8258(8) Å, γ = 90°	c = 12.6873(8) Å, γ = 90°
volume (Å^3)	2481.3(2)	2468.0(2)	2829.0(2)	1375.0(2)
Z	4	4	8	4
density (calc) (g/cm^3)	2.044	2.055	2.457	2.527
abs coeff (nm^{-1})	8.212	8.256	14.224	14.632
F(000)	1456	1456	1920	960
cryst size (mm)	0.54 × 0.36 × 0.26	0.40 × 0.26 × 0.14	1.02 × 0.27 × 0.14	0.60 × 0.46 × 0.14
θ range for data collection	1.29−28.26	1.28−28.25	2.52−28.29	3.00−28.14
index ranges	$-17 \le h \le 20$, $-14 \le k \le 13$, $-17 \le l \le 18$	$-21 \le h \le 16$, $-13 \le k \le 14$, $-18 \le l \le 18$	$-16 \le h \le 11$, $-18 \le k \le 17$, $-19 \le l \le 20$	$-12 \le h \le 17$, $-10 \le k \le 10$, $-16 \le l \le 15$
no. of reflns collected	14 887	14 894	16 047	7974
no. of ind reflns	5630 [R(int) = 0.0296]	5633 [R(int) = 0.0282]	3326 [R(int) = 0.1377]	3059 [R(int) = 0.1418]
no. of data/restraints/params	5630/0/299	5633/0/298	3326/0/148	3059/0/148
goodness-of-fit on F^2	0.882	1.068	0.914	1.070
final R indices [$I > 2\sigma(I)$][a]	R_1 = 0.0310, wR_2 = 0.1035	R_1 = 0.0320, wR_2 = 0.0693	R_1 = 0.0680, wR_2 = 0.1436	R_1 = 0.0602, wR_2 = 0.1493
R indices (all data)	R_1 = 0.0403, wR_2 = 0.1137	R_1 = 0.0413, wR_2 = 0.0738	R_1 = 0.1017, wR_2 = 0.1503	R_1 = 0.0744, wR_2 = 0.1598
largest diff peak and hole/e·Å^{-3}	0.851 and −0.874	0.816 and −1.097	3.180 and −5.745	2.719 and −2.081

[a] $R_1 = \sum(|F_o| - |F_c|)/\sum|F_o|$, $R_2 = \sum w_2(|F_o|^2 - |F_c|^2)^2$ where $w_2 = 1/(\sum|F_o|^2 + (0.0766((\max(F_o^2, 0) + 2|F_c|^2)/3)))$.

have no direct evidence for this, and thus a full structural analysis of the solid-state isomerization of **1** at different stages of the isomerization process is underway.

Experimental Section

The *diag* and *lat* isomers of **1** and **2** were prepared as previously described.[4,6] Suitable crystals were grown from CH_2Cl_2/hexanes mixtures at −15 °C. The X-ray data sets were collected on the 1K SMART Siemens CCD area detector system using Mo radiation. X-rays were generated using a regular sealed tube and an X-ray generator operating at 50 kV and 30 mA. The 9 cm wide CCD area detector was mounted 4.5 cm from the crystal and the data set collected at room temperature. A graphite monochromator followed by a 0.5 mm collimator was used. The selected crystal was mounted on a thin glass fiber.

To obtain an initial set of cell parameters and an orientation matrix for data collection, 183 (**1a**), 157 (**1b**), 139 (**2a**), or 74 (**2b**) reflections from three sets of 15 frames each were collected covering three perpendicular sectors of space. The data collection nominally covered more than a full sphere/hemisphere of reciprocal space, by a combination of three sets of exposures, 1271 frames. Each set had a different φ angle for the crystal, and each exposure covered 0.3° in ω, with 5 s exposure time per frame.

The final data set after internal scaling consisted of 14887 (**1a**), 14894 (**1b**), 16047 (**2a**), or 7974 (**2b**) reflections to 0.75 Å resolution. Coverage of all data is 91.6% (**1a**), 92.3% (**1b**), 98.93% (**2a**), or 92.18% (**2b**) complete to at least 28.26 (**1a**), 28.25 (**1b**), 28.30 (**2a**), or 28.14 (**2b**) in θ. The data collection took about 4 h. Details of the data collection and refinement are listed in Table 4.

The software package SHELXTLplus version 5.1[25] was used for space group determination, structure solution, and refinement. Molecular graphics were prepared using ORTEP3 for Windows[26] and PLATON.[27] The structures were solved by standard Patterson and Fourier techniques and refined by full-matrix least-squares methods based on F^2. The positional and anisotropic parameters for all non-H atoms were refined. The hydrogen atoms were placed in geometrically calculated positions and allowed to refine, riding on the atoms to which they are attached. Tables of calculated and observed structure factors for the structures have been deposited with the CCDC.

Acknowledgment. Funding from the FRD, THRIP, and University of the Witwatersrand is gratefully acknowledged.

Supporting Information Available: A listing of the atomic coordinates, bond lengths, bond angles, and torsion angles for the crystal structures of **1** and **2** is available. This material is available free of charge via the Internet at http://pubs.acs.org

OM990959Z

(25) Siemens *SHELXTLplus Version 5.1 (Windows NT version)—Structure Determination Package*; Siemens Analytical X-Ray Instruments Inc.: Madison, WI, 1998.
(26) Farrugia, L. J. *J. Appl. Crystallogr.* **1997**, 565.
(27) Speck, A. L. *PLATON, A Multipurpose Crystallographic Tool*; Utrecht University: Utrecht, The Netherlands, 1999.